Irradiation Creep of Zr-Alloys

M. Griffiths, G.A. Bickel, R. DeAbreu and W. Li

Abstract Irradiation creep of Zr-alloy nuclear reactor core components affects the reactor performance and also limits the reactor life in cases where those components cannot easily be replaced. For Zr-2.5Nb pressure tubing irradiation creep has been extensively studied for a range of temperatures, between 250 and 350 °C, and dose rates, between 1×10^{16} and 2×10^{18} n m^{-2} s^{-1} (E > 1 meV), using data from various materials test reactors and power reactors. These studies have shown that irradiation creep is controlled by a complex combination of slip and diffusional mass transport (often referred to as irradiation growth in the absence of stress). Irradiation creep is dependent on the crystallographic texture, the dislocation structure, and the grain structure; the importance of each being a function of irradiation temperature and displacement damage rate. Data will be presented, together with mechanistic modelling, to show what factors affect creep under different irradiation conditions.

Keywords Stainless steel · Thermal aging · Mechanical testing · Microstructure · Finite element method

Introduction

Irradiation creep of Zr-alloy nuclear reactor core components affects the performance of fuel cladding, fuel assemblies, guide tubes for reactivity mechanisms, and pressure tubes (in the case of CANDU and RBMK reactors). In-reactor gauging of pressurised components in power and materials test reactors have been conducted over many years in order to develop models that can be used in reactor design and for reactor life management. For Zr-2.5Nb pressure tubing in particular, irradiation creep has been extensively studied at CNL's Chalk River Laboratories (CRL) for a range of temperatures, between 250 and 350 °C, and dose rates, between 1×10^{16}

M. Griffiths (✉) · G.A. Bickel · R. DeAbreu · W. Li
Canadian Nuclear Laboratories, Chalk River, ON, Canada
e-mail: mal.com@bell.net

I. Charit et al. (eds.), *Mechanical and Creep Behavior of Advanced Materials*,
The Minerals, Metals & Materials Series, DOI 10.1007/978-3-319-51097-2_13

and 2×10^{18} n m^{-2} s^{-1} (E > 1 meV), using data from various materials test reactors and power reactors.

Work on creep capsules irradiated in OSIRIS and NRU has shown that two components of irradiation creep (dislocation slip and diffusion) are active and that the diffusional component dominates at high fast neutron fluxes, and by low temperatures (but not so low that recombination is dominant [1]). Irradiation creep is controlled by a complex combination of mechanisms based on dislocation slip, following the so-called climb and glide model [2, 3], and stress-modified diffusional mass transport [4, 5]. For a recent comprehensive review of creep mechanisms and creep models in Zr-alloys the reader is referred to the review by Adamson et al. [6] and a recent publication edited by Murty [7]. For Zr-alloys diffusional mass transport causes dimensional changes in reactor components in the absence of stress and is often referred to as irradiation growth. Zr-alloys are also anisotropic in their creep response and irradiation creep is dependent on the crystallographic texture, the dislocation structure, and the grain structure (size and shape) of the alloys [8–11], the importance of each being a function of irradiation temperature and displacement damage rate (given by the fast neutron flux). The data presented here, together with mechanistic modelling, are aimed at illustrating what factors affect creep under different irradiation conditions.

Creep of Zr-2.5Nb Pressure Tubing

Effect of Operating Conditions for a Given Microstructure

For this paper we focus on creep of Zr-2.5Nb pressure tubing. Much of the data for Zr-2.5Nb pressure tube comes from gauging of in-service pressure tubes. Because the tubes are long ($\sim$6 m) and there is a range of material variation along the tubes, as well as operating temperature and fast neutron flux, it is not possible to accurately assess the effects of operating conditions on axial creep. In order to fully assess the effects of temperature (T), flux and stress an both axial and diametral creep, controlled in-reactor tests need to be conducted. Recent data have been reported for small creep capsules irradiated in the NRU reactor at CRL and irradiated at relatively high temperatures (280–340 °C), which are just above the normal operating temperature range for CANDU pressure tubes (250–300 °C). The data were derived from two families of creep capsules, one with 12% cold-work and the other with 27% cold-work, all other microstructural variables (texture and grain structure) being more-or-less equal. The data have been reported previously [12] and here we present the statistical analysis using a generalised linear model given by the listed coefficients in Tables 1, 2, 3 and 4. The data have been normalised so the magnitude of the coefficient gives some measure of the significance of the variable or combination of variables in question. The *p*-value is a measure of the probability that the value is accurate; small *p*-values indicating high confidence in

Table 1 Axial strain rate

Effect	Coefficient	Standard error	*p*-value
CONSTANT	0.028	0.056	0.611
CW	0.067	0.055	0.229
STRESS	0.603	0.058	0.000
T	0.330	0.056	0.000
FLUX	0.746	0.057	0.000
T*STRESS	0.202	0.061	0.002
FLUX*T	0.086	0.058	0.143
T*CW	0.077	0.055	0.164

General linear model output for Zr-2.5Nb creep capsules irradiated in the NRU reactor showing the effect of the main operating variables on creep parameters for steady-state strain rate in the axial direction. The *p* value is the probability that the coefficient could be zero

Table 2 Diametral strain rate

Effect	Coefficient	Standard error	*p*-value
CONSTANT	0.038	0.049	0.449
CW	0.173	0.049	0.001
STRESS	0.469	0.052	0.000
T	0.650	0.050	0.000
FLUX	0.516	0.051	0.000
T*STRESS	0.295	0.054	0.000
FLUX*T	0.263	0.052	0.000
T*CW	0.132	0.049	0.008

General linear model output for Zr-2.5Nb creep capsules irradiated in the NRU reactor showing the effect of the main operating variables on creep parameters for steady-state strain rate in the axial direction. The *p* value is the probability that the coefficient could be zero

Table 3 Primary axial creep strain

Effect	Coefficient	Standard error	*p*-value
CONSTANT	0.017	0.097	0.858
CW	0.103	0.097	0.293
STRESS	0.202	0.102	0.051
T	0.237	0.098	0.018
FLUX	0.310	0.100	0.003
T*STRESS	0.051	0.107	0.633
FLUX*T	−0.441	0.101	0.000
T*CW	0.078	0.096	0.418

General linear model output for Zr-2.5Nb creep capsules irradiated in the NRU reactor showing the effect of the main operating variables on creep parameters for primary creep strain in the axial direction. The *p* value is the probability that the coefficient could be zero

Table 4 Primary diametral creep strain

Effect	Coefficient	Standard error	*p*-value
CONSTANT	0.008	0.058	0.893
CW	0.152	0.058	0.010
STRESS	0.318	0.061	0.000
T	0.433	0.058	0.000
FLUX	−0.584	0.060	0.000
T*STRESS	0.008	0.063	0.903
FLUX*T	−0.290	0.060	0.000
T*CW	0.017	0.057	0.762

General linear model output for Zr-2.5Nb creep capsules irradiated in the NRU reactor showing the effect of the main operating variables on creep parameters for primary creep strain in the diametral (hoop) direction. The *p* value is the probability that the coefficient could be zero

the coefficient. It is evident that the steady-state diametral creep rate is strongly dependent on fast neutron flux, temperature and stress plus combinations thereof, as one might expect. It is also evident that cold-working has a large effect. Whereas steady-state axial creep rates are also strongly dependent on fast neutron flux, temperature and stress, the cross terms with temperature are less significant (except perhaps for stress and temperature) and there is little apparent influence of cold-working. This is a surprising observation given that results at higher fluxes in OSIRIS show an effect of cold-work on axial but not diametral creep rates [8]. There are other ambiguities in the effect of up to 20% cold-work on irradiation defomation observed for Zralloy-2 [13]. It is evident that the primary diametral creep strain is strongly dependent on fast neutron flux, temperature and stress but the cross terms and cold-working have less significance compared with the steady-state behaviour. The primary axial creep strain is most sensitive to fast neutron flux and has little dependence on the degree of cold-work.

Focusing on the 27% cold-worked the results of applying a general linear model, with cross terms for temperature, flux and stress, are shown in Tables 5 and 6. It is evident that, whereas the cross term of flux and stress is significant for the axial

Table 5 Axial strain rate

Effect	Coefficient	Standard error	*p*-value
CONSTANT	0.085	0.043	0.054
STRESS	0.577	0.044	0.000
T	0.417	0.043	0.000
FLUX	0.715	0.043	0.000
T*STRESS	0.194	0.049	0.000
FLUX*STRESS	0.337	0.044	0.000
T*FLUX	0.119	0.044	0.010

General linear model output for Zr-2.5Nb creep capsules irradiated in the NRU reactor showing the effect of the main operating variables on the steady-state strain rate in the axial direction. The *p* value is the probability that the coefficient could be zero

Table 6 Diametral strain rate

Effect	Coefficient	Standard error	*p*-value
CONSTANT	0.055	0.059	0.355
STRESS	0.492	0.061	0.000
T	0.696	0.059	0.000
FLUX	0.510	0.060	0.000
T*STRESS	0.340	0.067	0.000
FLUX*STRESS	0.072	0.061	0.243
FLUX*T	0.262	0.061	0.000

General linear model output for Zr-2.5Nb creep capsules irradiated in the NRU reactor showing the effect of the main operating variables on the steady-state strain rate in the diametral (hoop) direction. The *p* value is the probability that the coefficient could be zero

strain rate, it is not for the diametral strain rate. The dependence on the product of neutron flux and stress is one of the basic tenets of irradiation creep [2, 3, 6, 7] and this lack of evidence for a cross-term dependence for diametral creep is somewhat surprising. One can reconcile this result with conventional creep models if one considers that at these elevated temperatures the dominant creep mechanism is not the same as that applicable at lower temperatures. Based on the evidence presented in [12] one can hypothesise that creep is dominated by dislocation slip at higher temperatures and low fast neutron fluxes, and by mass transport at lower temperatures and high fast neutron fluxes.

Effect of Microstructure for Normalised Operating Conditions

Models have been developed to describe the creep in 27% cold-worked Zr-2.5Nb pressure tubing [10, 11] that include texture as the main microstructural variable. Such models are mechanistically based on dislocation slip but fail to capture the material variability that exists due to the grain structure. Whereas creep by dislocation slip is expected to be adequately described using texture alone it has been long known that other material variables, in particular grain structure, need to be included. Early work used the existing models to normalise for operating conditions and the residuals correlated with easily measured grain structure parameters such as the minor axis grain dimension [15]. This parameter was used for expediency and gave a measure of the relative sink strength of grain boundaries (the boundary density) for point defects given that most of the grains tended to be flattened platelets with aspect ratios of 1:5–10:20–40 in the radial, transverse and axial direction respectively [16]. In principle, the strain realised from absorption of point defects at a grain boundary will be dependent on the combination of the tendency of a point defect to be migrating in a particular direction and the probability of encountering a boundary in the same direction. Thus, the intercept length for a given direction will be a function of the grain dimensions (thickness) and

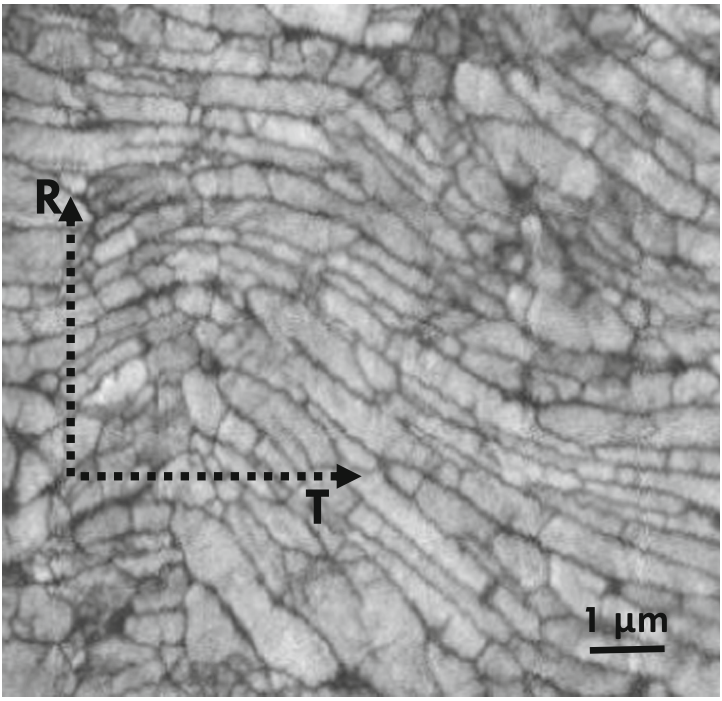

Fig. 1 Transmission Kikuchi diffraction band contrast image showing typical grain structure in Zr-2.5Nb pressure tubing. The grain boundary densities in the radial (R) and transverse (T) directions are derived from the intercepts along the *lines* shown

orientation. Figure 1 illustrates the complexity of a typical pressure tube grain structure. The sink densities for the radial and transverse directions are given by the intercepts with the radial and transverse directions as drawn. Figure 2 shows the correlation between radial and transverse grain intercept lengths and measured/predicted diametral strain using the same dataset as reported in [15], and normalised using the model described in [11].

The Zr-2.5Nb pressure tubes of a CANDU reactor have a length of about 6 m, an inner diameter of 104 mm and a wall thickness of 4.2 mm. During service, they operate with fast-neutron fluxes up to about 4×10^{17} n m^{-2} s^{-1} (E > 1 meV) coolant temperatures between 250 and 310 °C and coolant pressures up to 11.5 MPa, resulting in initial hoop stresses of about 140 MPa. The tubes expand subject to the stress, fast neutron flux, temperature and variable material creep rate, all of which vary along the length of the pressure tubes [16–20]. A large amount of gauging data are available for in-service Zr-2.5Nb pressure tubing and can be correlated with microstructural data from pressure tube offcuts with the application of a suitable normalisation model for the operating conditions [21]. The application of an empirical model that accounts for stress, fast neutron flux and temperature has made it possible to assess the effects of microstructural variables on diametral creep.

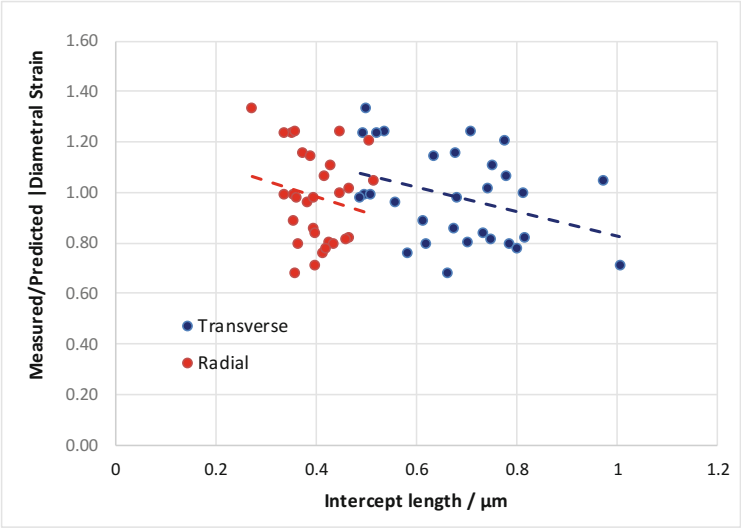

Fig. 2 Correlation between measured/predicted diametral strain and the transverse and radial intercept lengths for the back-ends of pressure tubes previously assessed in terms of minor axis grain dimension [15]

Data on texture, minor axis grain dimensions (thickness), grain aspect ratio and dislocation density have been compiled and assessed with respect to diametral creep. The results are shown for front and back-ends of pressure tubes in Tables 7 and 8.

Table 7 Model and statistics for multivariate fit—front-ends of Zr-2.5Nb pressure tubing

Summary statistics				
n (number of observations)				25
df (degrees of freedom)				20
R^2 (adjusted multiple-correlation coefficient)				0.6917
Model	Diametral strain residual $= \beta_0 + \beta_1 \cdot$ Aspect ratio $+ \beta_2 \cdot f_R$ $+ \beta_3 \cdot$ Radial grain thickness $+ \beta_4 \cdot$ Prism dislocation density where, Radial grain thickness is in units of μm and Prism dislocation density has units of $10^{14}/m^2$			
Parameter	**Value**	**se**	**τ**	**P(τ)**
β_0	−101	33	−3.09	0.0058
β_1	200	39	5.13	0.000051
β_2	284	70	4.06	0.00062
β_3	−91	32	−2.82	0.011
β_4	−10.7	4.2	−2.59	0.018

Se is the standard error and τ is the Student's t-value for the parameter being different from zero, *p(τ)* probability that τ could have its given value by chance

Table 8 Model and Statistics for Multivariate Fit -Back-ends of Zr-2.5Nb Pressure Tubing

Summary statistics				
n (number of observations)				25
df (degrees of freedom)				20
R^2 (adjusted multiple-correlation coefficient)				0.7494
Model	Diametral strain residual $= \beta_0 + \beta_1 \cdot$ Aspect ratio $+ \beta_2 \cdot f_R + \beta_3 \cdot$ Radial grain thickness $+ \beta_4 \cdot$ Prism dislocation density where, Radial grain thickness is in units of μm and Prism dislocation density has units of $10^{14}/m^2$			
Parameter	**Value**	**se**	**τ**	**P(τ)**
β_0	77	60	1.29	0.212
β_1	123	63	1.96	0.064
β_2	180	128	1.41	0.175
β_3	−435	88	−4.90	0.000087
β_4	−24.2	6.3	−3.81	0.0011

Se is the standard error and τ is the Student's t-value for the parameter being different from zero, *p(τ)* probability that τ could have its given value by chance

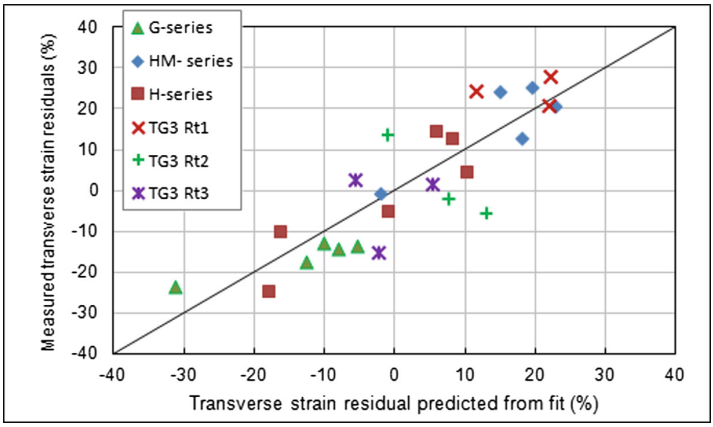

Fig. 3 Measured versus predicted transverse strain residuals predicted from the regression fit for bundle 3 (front) diametral strain. The *solid line* denotes measured = predicted

The results show that grain shape (aspect ratio) and texture are the most significant variables for the front-ends of Zr-2.5Nb pressure tubes. For the back-ends the grain minor axis dimension becomes increasingly significant. These statistical models show excellent agreement with measurement, as shown in Figs. 3 and 4.

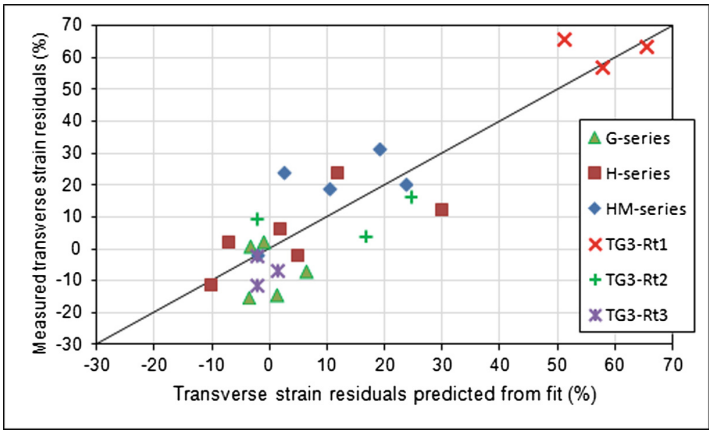

Fig. 4 Measured versus predicted transverse strain residuals predicted from the regression fit for bundle 11 (back) diametral strain. The *solid line* denotes measured = predicted

Effect of Impurities

Given that the pressure tubes are made from the Zr-2.5Nb binary alloy there are still impurities (notably oxygen and iron) that could influence creep. With the accumulation of more data, contrary to what was reported earlier [15], there is now little evidence to suggest that variations in oxygen affect diametral creep. Iron, on the other hand appears to have a negative correlation with diametral creep and axial elongation (Fig. 5) consistent with previous observations [17].

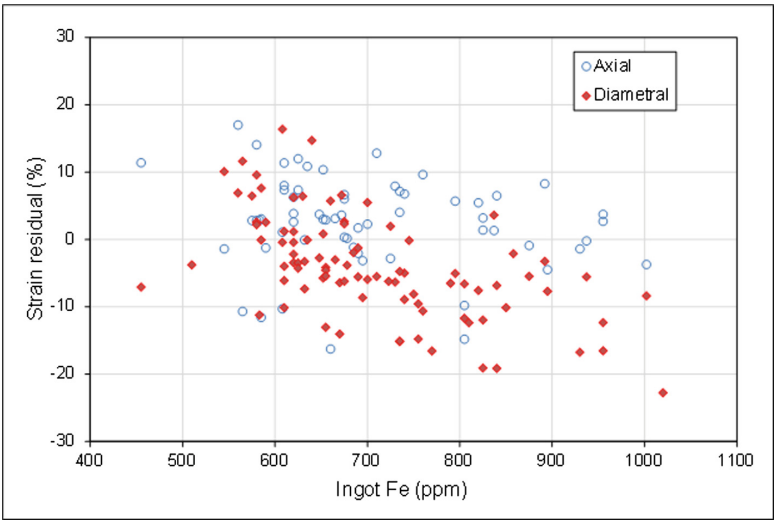

Fig. 5 Correlation between axial and diametral strain and Fe content in H-series tubes

Iron is both a ubiquitous and enigmatic in its possible effect on creep. Certain empirical correlations exist that show that Fe has the effect of decreasing irradiation creep in general. Whereas Fe may enhance the formation of c-component loops which could account for the lower diametral creep shown in Fig. 5 [21], the same effect would only enhance elongation [22]. The confounding effect of other microstructural variables has precluded any previous attempts to define what Fe does in terms of irradiation creep [17]. Without control of the microstructure one cannot be sure whether Fe has an effect on the microstructure as it develops during fabrication [17]. Fe stabilisation of c-component loops cannot account for the low elongation observed in Zr-2.5Nb pressure tubing (Fig. 5 and [17]) and the low elongation observed in other alloys where there is a strong axial prism texture [13]. The main role of Fe, if any, is therefore likely to be one of reducing mass transport. This can arise from enhancing recombination. Because Fe is an element that is thought to increase vacancy mobility [23, 24] it is unlikely that the effect on vacancy migration is the answer. One other possibility has been raised by Hood [25]. Hood has hypothesised that elements such as Fe, which can easily switch from substitutional to interstitial solid solution could aid in recombination, not by slowing down vacancies, but by an exchange with self-interstitials and subsequent annihilation at vacancies or other sinks. The effect of irradiation in general is to disperse Fe in the matrix [26] and Fe could then be effective in enhancing recombination, or simply reducing the self-interstitial concentration, thus inhibiting processes such as creep that depend on self-interstitial mass transport.

Discussion

Creep is generally considered to be a combination two mechanisms: (i) that due to dislocation slip (can be referred to as thermal creep whether in reactor or out-reactor), with a stress exponent $\neq 1$ (ii) that due to diffusion of point defects with a stress exponent =1. The stress-induced climb and glide model [2, 6, 7] consists of a rate-determining step governed by point defect diffusion to dislocations. This enables the dislocations to overcome barriers and glide until they encounter another barrier to motion—the slip is then an amplifier of the diffusion process. In that case the creep anisotropy cannot be dictated by the same factors affecting slip, e.g. the critical resolved shear stress. A clue comes from out-reactor creep—this is typically isotropic, whether or not the material has previously been irradiated [12]. Given that out-reactor thermal creep at reactor operating temperatures is widely accepted to be determined by dislocation slip it appears that this creep process is isotropic or nearly isotropic, which is quite different from the anisotropy displayed by yielding. The analyses shown in Tables 1, 2, 3, 4, 5 and 6 indicate that dislocation glide is likely to be an important contributor to creep at high temperatures and low fast neutron fluxes. When the temperature is low or the fast neutron flux is high it seems that a substantial portion of the creep is governed by diffusional processes. Other than some esoteric possibilities of grain boundary

sliding, the fact that grain boundaries have a strong influence on irradiation creep indicates that mass transport should be considered as the dominant mechanism at low stresses, high neutron fluxes and low temperatures. The main effect of grain structure on dislocation slip is to limit the maximum possible strain due to the annihilation of dislocations at grain boundaries and resulting in creep cessation. For Zr-2.5Nb pressure tubing and creep capsules with a strong transverse basal texture, and grains that tend to be flattened in the radial direction, creep due to dislocation slip will be exhausted for strains >1%. As creep capsules and pressure tubes are known to exhibit steady-state irradiation creep for strains in excess of 4% [3, 15–20], it is unlikely that the creep process is dominated by slip. Moreover, those pressure tubes exhibiting the highest diametral creep (referred to as TG3 RT1 in Fig. 4) were specifically manufactured to have a low dislocation density and small grain size [17]. With this in mind rate-theory models have been developed to explore the effects of microstructure on creep due to mass transport.

The strong dependence on grain size and aspect ratio observed for diametral creep of in-service pressure tubes suggests that a rate theory model [1] is an appropriate descriptor of the diametral creep behaviour. The neutron irradiation creates interstitials and vacancies that migrate to sinks such as dislocations, grain boundaries and in some cases cavities (neutral sinks). The net flux to a sink of a given orientation is determined by the difference in flow of interstitials and vacancies to those sinks, which can be calculated using:

$$J_m = \left(k_i^2\right)_m D_i C_i - \left(k_v^2\right)_m D_v C_v,$$

where m is the given type of sink and the subscripts i and v designate interstitials or vacancies respectively. The square of the average distance that a point defect migrates per second is given by D, and the average concentration in the matrix is C. The rate at which point defects migrate is given by the product, DC. The probability that a migrating point defect encounters a sink and therefore produces strain (positive for interstitials and negative for vacancies) is determined by the sink strength, k^2.

The sink strengths are relative and can be thought of as probabilities of encountering sinks of any one type when a point defect is migrating in a given direction. The strength is determined by the density and orientation of sinks and also, in the case of dislocations, the elastic interaction between the strain field around the sink and the point defects. As one is dealing with balance equations it is only necessary to be able to compute the relative strengths of the different sinks and these can be incorporated into the model as bias factors that account for the probability that a given sink has a propensity for absorbing interstitial, as opposed to vacancy, point defects. This enables the building of simple models to explore the interplay between various sinks and point defect properties. For example, one can represent the net flux to sinks resulting in strain in the radial (R), transverse (T) and longitudinal (L) directions of a pressure tube by the following expressions:

$$J_R = [(1 + (1 - f_R) \cdot p) \cdot D_i C_i - D_v C_v] \cdot (GB_R + \rho_R)$$
$$J_T = [(1 + f_R \cdot p + 2s) D_i C_i - D_v C_v] \cdot (GB_T + \rho_T)$$
$$J_L = [(1 + p + s) \cdot D_i C_i - D_v C_v] \cdot (GB_L + \rho_L)$$

where

$$D_i C_i = \frac{\phi}{(1 + (1 - f_R) \cdot p) \cdot (GB_R + \rho_R) + (1 + f_R \cdot p + 2s) \cdot (GB_T + \rho_T) + (1 + p + s) \cdot (GB_L + \rho_L)}$$

$$D_v C_v = \frac{\phi}{(GB_R + \rho_R) + (GB_T + \rho_T) + (GB_L + \rho_L)}$$

The grain boundary and dislocation sink densities corresponding with each direction *R*, *T* and *L* are given by GB_m and ρ_m, where the orientation, m = *R*, *T* and *L*. In this model the interstitial bias factor [14], p, is assumed to be a function of sink orientation and interstitial diffusional anisotropy. The bias parameter is modified by the basal pole orientation parameter, f_R, in order to capture the effect of the diffusional anisotropy difference of interstitial point defects along the **a** and **c**-axes [27]. An additional bias due to stress, s, is applied to interstitial diffusion based on the concept of the influence of stress on diffusion [28], and developed as the "elastodiffusion" model for creep by Woo [29]. The sink densities, GB_m and ρ_m, can be separated with appropriate changes of bias factors to account for strain-field interactions if necessary. It is easy to see that: $J_R + J_T + J_L = 0$.

One can then investigate how varying the grain boundary sizes and shapes affects the diametral creep while holding the texture and dislocation density constant for each grain.

Although the sink density in a given direction is determined by the intersection with grain boundaries of various orientations one can model the resultant effect by assuming an effective grain whose dimensions correspond with the average intercept length for the main component directions. Figure 6 shows the effect of varying the grain shape on strain in the three principle directions of a pressure tube or creep capsule. Each condition considered (B and C) exhibits less total strain compared to the nominal condition (A) with typical aspect ratios of 1:10:40 in the radial, transverse and axial directions respectively [16]. Figure 7 shows the worst condition for maximum diametral strain, i.e. when the grain is close to being equiaxed in the radial and transverse directions.

There is a strong interplay between the absolute and relative dimensions of the grain structure that affects the predicted creep strain. Having smaller grain dimensions (thinner grains) enhances the relative effect that grain structure has in controlling creep, i.e. grain boundaries are stronger sinks for point defects compared with dislocations that are assumed to have a constant density. Ultimately the net strain is dictated by the partitioning of the interstitial and vacancy point defects to different sinks. If the sink capture volume for both types of defects overlap [1] there will be no net strain. This would be a situation where the sink density is very

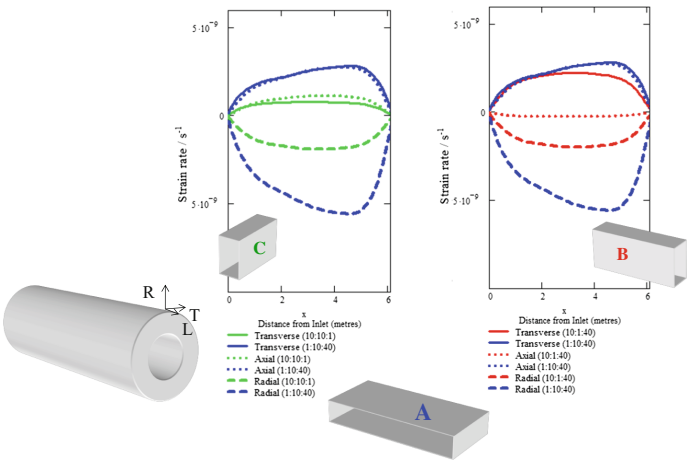

Fig. 6 Effect of different grain shapes on strain calculated using a rate-theory model containing grain dimensions (see text). The effect of aspect ratio for the R, T and L directions is illustrated. The outlet is at the 6 m location to the right of each plot. The *blue curves* are hypothetical strain profiles along a pressure tube in a CANDU reactor where the grain structure is idealised as thin platelets similar to A. The total strain can be minimised with a grain shaped as in C, where the minor axis dimension is parallel with the longitudinal axis of the tube. The axial strain is negative with grain shape B (Color figure online)

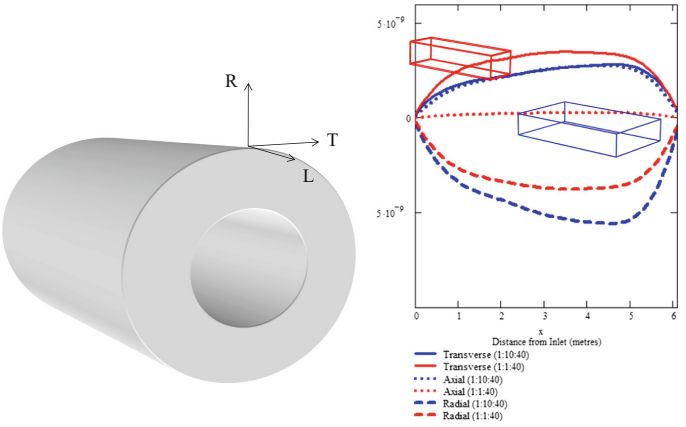

Fig. 7 Effect of different grain shapes on strain calculated using a rate-theory model containing grain dimensions (see text). The outlet is at the 6 m location to the right of each plot. The blue curves are hypothetical strain profiles along a pressure tube in a CANDU reactor where the grain structure is idealised as thin platelets (the normal grain structure). The highest diametral creep is adjusted for grains having small and similar radial and transverse dimensions

high, for example with a nano-scale grain size. When the sink density is sufficiently low that biased flow can operate the optimum condition for maximum strain occurs when the partitioning of vacancies and interstitials to different sinks is balanced. This occurs when the product of the bias and sink density for different vacancy and interstitial sinks are equal. Assuming that elastodiffusion operates [29] then the maximum diametral creep can be expected when the product of the interstitial bias and sink strength for interstitial diffusion in the transverse direction is equal to the product of the sink strength and vacancy bias for vacancy diffusion in the radial direction. Assuming that there is no directional bias for vacancy diffusion, i.e. the effect of texture and stress is manifested by the effect on interstitial diffusion, then the optimum condition occurs when the product of the sink density and bias for interstitial flow is equal to the unbiased sink density (for net vacancy sinks). There will thus be an optimal grain shape that maximises diametral strain dictated by the bias for interstitial flow in the transverse direction (governed by the texture and stress). As pressure tubes contain network dislocations that compete for point defects (net interstitial bias) reducing the magnitude of the grain dimensions that increases the overall grain boundary sink strength will result in a response that is dictated more by grain structure and less by texture.

With respect to the data presented in Tables 7 and 8 the grain structure has a strong effect on diametral creep. As the net point defect flow in any one direction is balanced by the net flow in other directions it is easiest to explore the effect of microstructural variation using the rate-theory model described here. Treating the average intercept length in any one direction as a surrogate grain dimension, Fig. 8 shows that there is a tendency for higher diametral creep when the grain dimensions in the radial and transverse direction are similar. When elastodiffusion is prominent there is a tendency to have increased diametral creep when the grains are more flattened in the radial direction (Fig. 8a) and this effect is enhanced when the dislocation density is reduced (Fig. 8b). The effect of reducing the hoop stress is shown in Fig. 9. Reducing the stress-induced bias means that the response is less

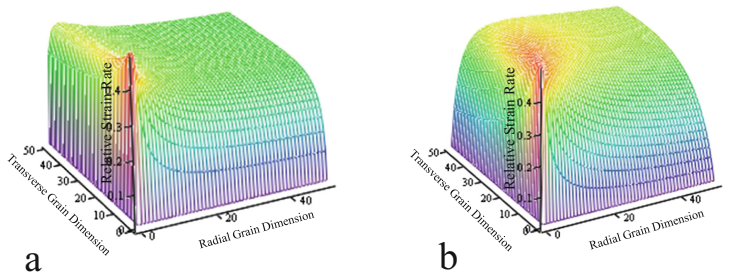

Fig. 8 Rate-theory model output showing the effect of varying grain dimensions on the relative diametral strain rate. In this example the elastodiffusion or stress bias is large. The dislocation density sink strength is comparable to that of the grain boundaries in (**a**) and is reduced by a factor of 10 in (**b**)

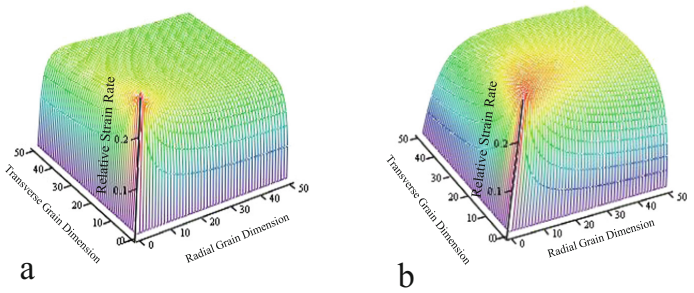

Fig. 9 Rate-theory model output showing the effect of varying grain dimensions on the relative diametral strain rate. In this example the elastodiffusion or stress bias is small. The dislocation density sink strength is comparable to that of the grain boundaries in (**a**) and is reduced by a factor of 10 in (**b**)

dependent on the radial minor axis dimension and more dependent on having equiaxed grains when viewed down the longitudinal axis of the tube.

The driving force for producing strain is the interaction between point defects that tend to migrate in a particular direction with sinks that have a high density along that direction. Creep due to mass transport will be the dominant mechanism when the grain boundary sink strength is high relative to the dislocation sink strength. Conversely, dislocation slip will dominate when the grain size is large. Smaller grains will limit the contribution from dislocation slip because the gliding dislocations will eventually annihilate at the boundaries resulting in creep cessation. Because irradiation creep is higher for small-grained material (as appears to be the case in pressure tubes operating at 250–300 °C) then it is likely that mass transport is the dominant process. The creep component dictated by dislocation slip is also likely to dominate at high stresses and high temperatures because creep below yield by dislocation slip is a thermally activated process whereas irradiation creep in a sink-dominate regime is relatively unaffected by temperature, the rate-determining step being the point defect production.

The external factors that control the creep-rate are primarily stress-state and temperature. There are a number of material factors that are important and these can change as the microstructure evolves, both with and without irradiation. Apart from alloying additions, the main material factors affecting creep are residual stresses, texture, dislocation density and grain structure. One cannot study the effect of any one factor without maintaining the others constant (as much as possible). With regards to residual stress, a simple stress-relief treatment will help minimise the impact. With regards to texture, dislocation density and grain structure it is often very difficult to increase the range of one of these variables without affecting the other two and therefore one must rely on multi-variable analysis to determine the relative contributions of each. We have thus studied the dependence of irradiation creep on microstructure using a multi-variable analysis of the residuals after

applying an empirically derived equation to the data that normalises for the effect of operating conditions [21].

Conclusions

Irradiation creep is determined by both dislocation slip and mass transport in Zr-2.5Nb pressure tubing. For conditions where the contribution from dislocation slip is minimal (moderate fast neutron flux at low temperatures, <300 °C) the creep is dictated by crystallographic texture and grain structure. Mass-transport is the dominant creep mechanism at normal power reactor operating temperatures (250–300 °C) and at high fast neutron fluxes (>10^{17} n m^{-2} s^{-1}). Creep is dominated by dislocation glide at higher temperatures and lower fluxes.

Acknowledgements The authors would like to thank Clinton Mayhew for generating the TKD image. Partial funding for this work was provided by the Candu Owners Group (COG).

References

1. P.T. Heald, M.V. Speight, Point defect behaviour in irradiated materials. Acta Metall. **23**, 1389 (1975)
2. F.A. Nichols, Radiation-enhanced Creep. ERDA R&D Report WAPD-T-2636, bettis Atomic Power Laboratory (1975)
3. R.A. Holt, In-reactor deformation of cold-worked Zr-2.5Nb pressure tubes. J. Nucl. Mater. **372**, 182–214 (2008)
4. C.H. Woo, Theory of irradiation deformation in non cubic metals effects of anisotropic diffusion. J. Nucl. Mater. **159**, 237–256 (1988)
5. C.H. Woo, in *Effects of Anisotropic Diffusion on Irradiation Deformation*, ed. by F.A. Garner, N.H. Packan, A.S. Kumar, Proceedings of the 13th International Symposium on Radiation-Induced Changes in Microstructure, ASTM STP 955, ASTM International, Philadelphia, PA, 1987, pp. 70–89
6. R.B. Adamson, F. Garzarolli, C. Patterson, *In-reactor creep of zirconium alloys* (ANT International, Molnlycke, Sweden, 2009)
7. K.L. Murty (ed.), Elsevier, Materials ageing and degradation in light water reactors: mechanisms and management—technology & engineering. Woodhead Publishing Series in Energy (2013). ISBN 0857097458 and 9780857097453
8. L. Walters, G.A. Bickel, M. Griffiths, *The Effects of Microstructure and Operating Conditions on Irradiation Creep of Zr-2.5Nb Pressure Tubing*, ed. by R.J. Comstock, P. Barbéris, Proceedings of the 17th International Symposium on Zirconium in the Nuclear Industry, ASTM STP 1543, ASTM International, West Conshohocken, PA, 2014, pp. 693–722
9. A.R. Causey, J.E. Elder, R.A. Holt, R.G. Fleck, *On the Anisotropy of In-Reactor Creep of Zr-2.5Nb Tubes*, ed. by A.M. Garde, E.R. Bradley, Proceedings of the 10th International Symposium on Zirconium in the Nuclear Industry, ASTM STP 1245, ASTM International, Philadelphia, PA, 1994, pp. 202–219

10. A.R. Causey, R.A. Holt, N. Christodoulou, E.T.C. Ho, *Irradiation-Enhanced Deformation of Zr-2.5Nb Tubes at High Neutron Fluences*, ed. by G.P. Sabol, G.D. Moan, Proceedings of the 12th International Symposium on Zirconium in the Nuclear Industry, ASTM STP 1354, ASTM International, West Conshohocken, PA, 2000, pp. 74–84
11. N. Christodoulou, A.R. Causey, R.A. Holt, C.N. Tome, N. Badie, R.J. Klassen, R. Sauve, C. H. Woo, *Modelling In-Reactor Deformation of Zr-2.5Nb Pressure Tubes in CANDU Power Reactors*, ed. by E.R. Bradley, G.P. Sabolm, Proceedings of the 11th International Symposium on Zirconium in the Nuclear Industry, ASTM STP 1295, ASTM, West Conshohocken, PA, 1996, pp. 518–537
12. R.F. DeAbreu, G.A. Bickel, A.W. Buyers, S.A. Donohue, K. Dunn, M. Griffiths, L. Walters, *Temperature and Neutron Flux Dependence of In-Reactor Creep for Cold-worked Zr 2.5Nb*, ed. by R.J. Comstock, A. Motta, Proceedings of the 18th International Symposium on Zirconium in the Nuclear Industry, ASTM International, West Conshohocken, PA, 2016
13. S. Yagnik, R. Adamson, G. Kobylyansky, J.H. Chen, D.r Gilbon, S. Ishimoto, T. Fukuda, L. Hallstadius, A. Obukhov, S. Mahmood, *Effect of Alloying Elements, Cold Work, and Hydrogen on the Irradiation-Induced Growth Behavior of Zirconium Alloy Variants*, ed. by R.J. Comstock, A. Motta, Proceedings of the 18th International Symposium on Zirconium in the Nuclear Industry, ASTM International, West Conshohocken, PA, 2016
14. K.L. Murty (ed.), Elsevier, Materials ageing and degradation in light water reactors: mechanisms and management—technology & engineering. Woodhead Publishing Series in Energy (2013). ISBN 0857097458 and 9780857097453
15. M. Griffiths, W.G. Davies, G.D. Moan, A.R. Causey, R.A. Holt, S.A. Aldr*idge, Variability of In-reactor Diametral Deformation for zr-2.5Nb Pressure Tubing*. 13th International Symposium on Zirconium in the Nuclear Industry, ASTM STP 1423, American Society for Testing and Materials, pp. 796–810
16. G.A. Bickel, M. Griffiths, Manufacturing variability, microstructure and deformation of Zr-2.5Nb pressure tubes. J. ASTM Int. **4**(10) (2007) (Paper ID JAI101126)
17. G.A. Bickel, M. Griffiths, Manufacturing variability and deformation for Zr-2.5Nb pressure tubes. J. Nucl. Mater. **383**(1–2), 9–13 (2008)
18. D.K. Rodgers, C.E. Coleman, M. Griffiths, G.A. Bickel, J.R. Theaker, I. Muir, A.A. Bahurmuz, S.St Lawrence, M. Resta Levi, In-reactor performance of pressure tubes in CANDU reactors. J. Nucl. Mater. **383**(1–2), 22–27 (2008)
19. G.A. Bickel, M. Griffiths, A. Douchant, S. Douglas, O.T. Woo, A. Buyers, *Development of Zr 2.5Nb Pressure Tubes for Advanced CANDU Reactor*. Sixteenth International Symposium on Zirconium in the Nuclear Industry, Chengdu, China, June 2010
20. D.K. Rodgers, M. Griffiths, G.A. Bickel, A. Buyers, C.E. Coleman, H. Nordin, S. St. Lawrence,In-reactor performance of pressure tubes in CANDU reactors. AECL Nucl. Rev. **5** (1) (2016). doi:http://dx.doi.org/10.12943/CNR.2016.00007
21. M.I. Jyrkhama, G.A. Bickel, M.D. Pandey, Statistical analysis and modelling of in-reactor diametral creep of Zr-2.5Nb pressure tubes. Nucl. Eng. Des. **300**, 241–248 (2016)
22. M. Griffiths, R.A. Holt, A. Rogerson, Microstructural aspects of accelerated deformation of zirconium alloy nuclear reactor components. J. Nucl. Mater. **225**, 245 (1995) (Proc. 16th Int. Symp. on the Effects of Irradiation on Materials (1995))
23. G.M. Hood, *The Vacancy Properties of Al and alpha-Zr*, ed. by S. Saimot, G.R. Purdy, G.V. Kidson, Proceedings of the International Seminar on Solute-Defect Interaction, Theory and Experiment, Pergamon Press, Toronto, 1986, pp. 83–90
24. G.M. Hood, *Point Defect Diffusion in alpha-Zr*, ed. by C.H. Woo, R.J. McElroy, Proceedings of the International Conference on Fundamental Mechanisms of Radiation-Induced Creep and Growth (Elsevier Science Publishers B.V., North-Holland–Amsterdam, 1988), pp. 149–175
25. G.M. Hood, Point Defect properties of α-Zr and their Influence on Irradiation Behaviour of Zr-alloys, AECL-5692 (1977)
26. M. Griffiths, J.F. Mecke and J.E. Winegar, *Evolution of Microstructure in Zirconium Alloys during Irradiation*. Proceedings of 11th International Symposium on Zr in the Nuclear Industry, Garmisch, Germany, Sept. 1995, ASTM STP 1295 (1996), p. 580

27. C.H. Woo, U. Gosele, Dislocation bias in an anisotropic diffusive medium and irradiation growth. J. Nucl. Mater. **119**, 219–228 (1983)
28. P.H. Dederichs, K. Schroeder, Anisotropic diffusion in stress fields. Phys. Rev. B **17**, 2524–2536 (1978)
29. C.H. Woo, Irradiation creep due to elastodiffusion. J. Nucl. Mater. **120**, 55–64 (1984)